Astron. Astrophys. 303, L9–L12 (1995)

ASTRONOMY AND ASTROPHYSICS

Letter to the Editor

On the generation of loop-top impulsive hard X-ray sources

L. Fletcher

Sterrekundig Instituut, P.O. Box 80 000, 3508 TA Utrecht, The Netherlands

Received 15 August 1995 / Accepted 12 September 1995

Abstract. Recently observed with the Hard X-ray Telescope onboard Yohkoh, loop-top hard X-ray sources have focussed interest on energy release in solar flares. Possibly a direct indication of the site of particle acceleration, they have thus far only been interpreted as thermal sources. In this letter we propose instead that the sources arise as a result of transport effects, and show using a stochastic simulation of non-thermal electron transport in a simple loop model, that many characteristics of the loop-top source can be reproduced.

Key words: sun:flares, corona, particle transport, X-rays.

1. Introduction

On 13 January 1992, the Yohkoh satellite made observations of a large flare occurring near the solar limb (Masuda *et al.* 1994). These showed quite clearly two well resolved bright hard X-ray sources, almost coincident with the footpoints of a soft X-ray emitting loop, and a remarkable, bright, also well-resolved, hard X-ray source, apparently located above the apex of the soft X-ray emitting loop. Further observations (Masuda 1994) revealed more of these sources, located at or above the apex of SXR loops, during the impulsive phases of compact solar flares. They have become known as 'loop-top impulsive hard X-ray sources', and potentially provide direct information about the site and nature of particle acceleration in compact solar flares. The time evolution of the sources follows closely that of the footpoint hard X-ray sources, the intensity is about a factor five lower, and the spectral index (as far as it can be determined from the four energy bands of the HXT) tends to be higher than that of the footpoints, i.e., the spectra are steeper. The sources are compact: in the 13 January flare most of the emission in the 33-53 keV energy band originated in a region of linear dimension about 2×10^8cm, small compared to the typical compact loop length of about 10^9cm.

Send offprint requests to: L. Fletcher

The model suggested by Masuda *et al.* is that loop-top hard X-rays are thermal bremsstrahlung from a 'super-hot' plasma of density $\sim 10^8 \mathrm{cm}^{-3}$ at the loop top, shock heated by a reconnection flow emanating from Y-type reconnection point located above the loop. Electrons which precipitate to cause the footpoint emission are either part of the loop-top population, or are created in parallel with the super-hot plasma at the shock but were never part of the population responsible for the loop-top source. But if there is a super-hot source at the loop-top, continually being heated by reconnection flows, and possibly 'feeding' the footpoint sources, we have to ask how it might be contained. The plasma should expand down the loop legs at a few times the ion-acoustic speed $c_s = (kT/m_i)^{1/2}$ or a few times $9 \times 10^7 \mathrm{cms}^{-1}$ in a 10^8K plasma. So in a few seconds the source should double in size, a phenomenon which is not observed (Masuda, private communication), by which we would have to infer that the super-hot plasma is somehow contained in this model.

As an alternative, we investigate the possibility that the loop-top source is a non-thermal feature generated by electron transport, rather than being thermal emission from a super-hot plasma.

2. Non-thermal emission.

2.1. The model

We model the environment in which the hard X-rays are produced as a semi-circular magnetic loop, anchored in the photosphere, which in the corona (heights greater that 2×10^8cm above the photosphere) has a uniform cross-section, ambient density and magnetic field. In the chromosphere the field converges according to a form proposed by MacKinnon and Brown (1990) in which $\nabla.\mathbf{B} = 0$. The chromospheric density increases downwards - according to an exponential density law with a fixed photospheric density ($9.23 \times 10^{16} \mathrm{cm}^{-3}$) corresponding to that found by an exponential fit to the flare model atmosphere F2 of Machado *et al.* (1980). The coronal density is determined by the chromospheric value at 2×10^8cm above the photosphere, and density is varied by changing the chromospheric scale-height. The electron distribution is injected

at the top of the loop, at a single position, an assumption which is justified by the small spatial extent of the loop-top source compared with the loop length. This allows us to separate the spatial effects of transport from those of injection.

2.2. The evolution of the energetic electron distribution.

The emitted X-ray emission at a given position is determined by the local non-thermal electron distribution as well as the 'background' plasma density. Including Coulomb energy loss, pitch angle scattering and magnetic mirroring in the description of the evolution of the non-thermal electron distribution results in a complex evolution equation which in general cannot be solved analytically. We use a numerical method (stochastic simulations) to describe how the particle distribution function evolves, and from the distribution function we calculate the HXR emission.

The evolution equation for the distribution function f, as a function of energy E, velocity v, pitch angle cosine μ and coordinate z along the magnetic axis is

$$\frac{\partial f}{\partial t}+\mu v\frac{\partial f}{\partial z}-\frac{4\pi e^4\Lambda n}{m_e v}\frac{\partial}{\partial E}\left(\frac{f}{v}\right)-\frac{v}{2}\frac{\partial}{\partial \mu}\left((1-\mu^2)\frac{dlnB}{dS}f\right)$$

$$-\frac{4\pi e^4\Lambda n}{m_e^2 v^3}\frac{\partial}{\partial \mu}\left((1-\mu^2)\frac{\partial f}{\partial \mu}\right)=0 \qquad (1)$$

where n is the local particle density, e, m_e the electron charge and rest-mass, Λ the Coulomb logarithm and B the local magnetic field. This is a Fokker-Planck (diffusion-advection) equation, and it has been demonstrated by Gardiner (1985) that this type of equation is strictly equivalent to a set of stochastic differential equations, describing the time evolution of each component of the particle velocity vector. The equations for the increment of each variable in this case are

$$\begin{aligned}
\Delta z &= \mu v\Delta t,\\
\Delta v &= \frac{-4\pi e^4\Lambda n}{m_e^2 v^2}\Delta t,\\
\Delta \mu &= \left[\frac{-8\pi e^4\mu\Lambda n}{m_e^2 v^3}-\frac{v}{2}(1-\mu^2)\frac{\partial lnB}{\partial z}\right]\Delta t,\\
&+\left[\frac{4\pi e^4\Lambda n}{m_e^2}\frac{(1-\mu^2)}{v^3}\right]^{1/2}\Delta W(t).
\end{aligned}$$

The term $\Delta W(t)$ has the dimension of time and is a Wiener process of mean zero and variance 2, which scales as $(\Delta t)^{1/2}$. In practice it is a number drawn at random from a suitable Gaussian distribution, (since Coulomb scattering, a random walk process, gives a distribution which is nearly Gaussian in nature, except that it cannot extend to infinity). So if we choose many values of $\Delta W(t)$, and scale by the local collisional diffusion coefficient, we generate a distribution which accurately represents the pitch-angle cosine distribution of electrons undergoing Coulomb collisions, after a timestep Δt. We construct the particle distribution from many realisations of individual particle trajectories, governed by these equations. At each scattering the particle energy and position is also updated, along with the background plasma and field values. To build up a distribution with reliable statistics we simulate the trajectories of typically 120,000 particles. The particles move down the loop towards the chromosphere, scattering as they go, and in the chromosphere they either precipitate out, losing all their energy to Coulomb collisions, or mirror in the convergent field and return to the corona. Particles returning past the point of injection reappear in the simulation with their velocity mirrored in the loop axis, which is equivalent to their passing into the other leg of the loop. The final result is thus an average over both loop legs. The results of the simulation are integrated over a particle lifetime (the order of seconds). Observed time variability can be obtained by time-varying flux injection, provided that the typical timescale of injection is larger than the particle lifetime.

We have not included the effects of deceleration of test electrons in the field of a beam-generated return current, or due to anomalous resistivity, and this limits the range of coronal densities and temperatures to which the model applies. According to van den Oord (1990) the primary energy losses are collisional if $v < (n_b/n)^{1/3}v_{th}$, and anomalous resistivity sets in if $v > (n_b/n)c_s$ where n_b is the beam density, v_{th} is the electron thermal speed and c_s is the ion acoustic speed. If we assume that the total energy released in the flares associated with looptop sources is 10^{31} ergs (reasonable for M-type flares, as the observed flares are) over a timescale of 5 minutes, and assume also that the majority of this energy is in the form of a beam which covers a chromospheric area of 10^{18}cm^2 we require an energy flux of 3.3×10^{10}ergscm^{-2}s^{-1}. If we have a power-law distribution of electrons extending from 20keV to infinity, then the required beam density is a few times 10^8 electrons cm^{-3}, for flux power law indices between 3.5 and 6.5. Therefore, for the ambient densities which we shall consider, $3\times10^{10}-3\times10^{11}$ electrons cm^{-3}, the beam (20 - 200 keV) is in the Coulomb collision-dominated regime for plasma temperatures of a few times 10^7 K, which is quite reasonable for coronal plasmas.

Note that this method has already been used in a number of solar and astrophysical applications, to which the reader is referred for futher explanation (eg MacKinnon and Craig 1992, Fletcher and Brown 1995, Achterberg and Krülls 1992).

2.3. Emission of HXR radiation

For electrons of energies below 150 keV it is adequate to employ the Bethe-Heitler cross section for Bremsstrahlung

emission. The total position - dependent HXR emission is calculated by numerically evaluating the integral

$$I(\epsilon, z) = \int_{\epsilon}^{\infty} \int_{-1}^{1} f(z, E, \mu) n_p(z) \sigma(\epsilon, E) d\mu dE \qquad (2)$$

where ϵ is the energy of the emitted radiation.

3. Results

In figure 1 we show calculated flux maps of HXR emission generated along one half of the loop (the other half is a mirror image) at energies of 30 and 50keV. At energy lower than 20keV there may well be contamination by thermal emission from the loop, therefore we do not make a comparison with the observations on the basis of a purely non-thermal model. We have used a coronal loop density of

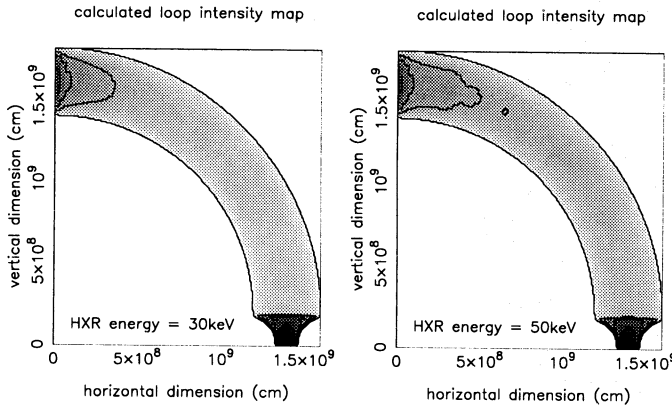

Fig. 1. The maps obtained at 30keV and 50keV for an isotropic injection of electrons into a loop of density $3 \times 10^{10}\mathrm{cm}^{-3}$, convergent in the chromosphere.

$3 \times 10^{10}\mathrm{cm}^{-3}$, a field structure which converges high up in the chromosphere, with photospheric field strength 1000G and coronal field strength 100G, and an isotropic particle distribution with a power-law distribution in electron flux $F(E) = F_o E^{-\delta}$ with $\delta = 3$. The grey scale represents the product of intensity and tube thickness (depending on distance from tube axis) giving a number which can be compared to the line-of-sight HXR flux. We have assumed that the electrons are injected steadily and uniformly across the tube cross section. (Note that in more detailed modelling, the radial variation of the electron distribution and hence the HXR intensity should be calculated, to enable better comparison with the HXR contours across as well as along the loop.) The grey scale is normalised to the maximum flux in each figure, and the contours are at 70%, 50%, 35% and 25% of the maximum. This enables comparison with the normalised HXT countours. In calculating the HXR intensities we take into account the conservation of total electron flux along the tube, so that the local density of 'test' electrons and hence the intensity of their HXR emission is enhanced in narrow tube regions, by a factor $(r(z)/r_{max})^2$.

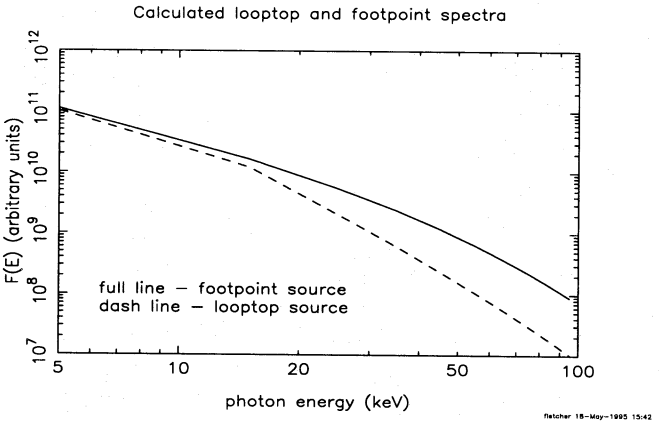

Fig. 2. loop-top and footpoint spectra for the emission plotted in figure 1.

At both 30 and 50 keV there are quite clearly patches of high intensity X-ray emission at the loop-top, as well more intense footpoint sources. For this isotropic pattern of injection, the source is slightly larger at high energy than at low energy. If we calculate the spectra we find that the loop-top source is slightly softer than the footpoint source, and a factor 5 to 10 less intense. Both the spectral index and the intensity depend on the energy band. At around 25 keV the spectral index of the footpoint is $\gamma \sim 2.1$, indicating thick-target emission (particles lose energy through Coulomb collisions as they emit) as the spectral index γ is one less than the spectral index δ of the injected flux distribution, which had $\delta = 3$. The loop-top source has $\gamma = 3.4$, indicating that the emission is not entirely thin target emission, for which the spectral index is one softer than for the injected flux distribution (i.e., $\gamma = 4$). At high energy, the power law indices change - the emission becomes softer in both cases, since the energy losses of electrons are smaller at high energy, and the emission is more like thin-target. The loop-top spectrum is calculated from emission in the region between 0 and 3×10^8cm from the top of the loop, and the footpoint spectra uses all points in the chromosphere.

The presence of loop-top emission can be simply explained. Electrons injected at the top of the loop with large pitch angle do not progress quickly down the loop - instead they remain near the loop-top orbiting the field until they are sufficiently scattered by Coulomb collisions, and begin to move preferentially along the field. Whilst at the loop-top they emit HXR bremsstrahlung, and since the scattering timescale is of order the energy loss timescale for electrons undergoing Coulomb collisions, the electrons also lose some energy collisionally, and the emission has

a spectrum which is between thick and thin target. The emission thins out along the tube as the average velocity of non-thermal electrons parallel to the tube increases (as they scatter into the parallel direction) and by conservation of flux the local density decreases.

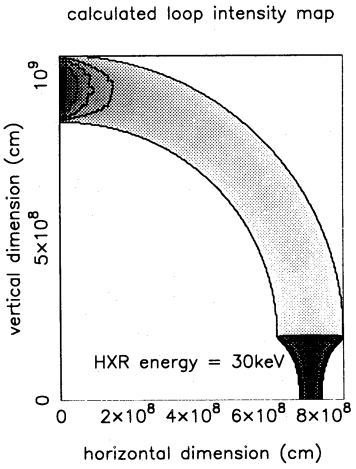

Fig. 3. The map of HXR intensity at 30keV for a background particle density of $3 \times 10^{11} \mathrm{cm}^{-3}$. The loop-top source is more intense than at lower densities.

If the density in the loop is increased, the intensity of the loop-top source grows, since the electrons have relatively more encounters in the denser corona which resulting in bremsstralung hard X-rays. The loop-top spectrum also becomes harder, and loop-top emission begins to dominate over footpoint emission at low energy as the loop density increases.

Note that it is a prediction of this model that the loop-top source will never be harder than the footpoint source, since the footpoint source is mainly due to thick-target emission (at least at low energies), whilst the loop-top source will be 'semi-thick' - i.e., some of the particles' energy is lost collisionally as they radiate.

4. Discussion

We have shown that a loop-top source arises naturally from a non-thermal model of electron bremsstrahlung emission of hard X-rays, with spectral and spatial characteristics consistent with what is observed.

The simulations presented here are rather simplistic and rather crude in that they do not take into account the dependence of emission on the radial co-ordinate in the tube, which is necessary to do a proper line-of-sight integration of the hard X-ray intensity. Nor do they account for possible variations in target density along the loop, or anisotropic injected distributions. Such studies are necessary to explain in detail the shape of the contours seen at various energies. For example, we have shown here that if particles are injected isotropically, with no variation of energy with pitch angle, the low energy source is smaller than the high energy source. However, we have found (although it is not shown here) that if pitch angle at injection increases with increasing electron energy, the source is larger at low energy than it is at high energy. Still, even with our crude model we have demonstrated that it is not necessary to invoke a thermal emission from a super-hot plasma to explain the presence of a hard X-ray loop-top - a non-thermal model including appropriate transport effects will also do the job. Note that a prediction of this model is that the spectral index of the loop-top source will consistently be larger than of the footpoint source.

The position of the source is centered on the site of injection or acceleration of electrons into the loop - for example at a shock site in the same kind of geometry as suggested by Masuda *et al.* Therefore much in the same way as these authors suggest, the loop-top source could appear above a separate soft X-ray loop, which is filled with evaporated plasma from the chromosphere already heated by electron bombardment.

Given the results of our model based on non-thermal electron bremsstrahlung, the excitement of the loop-top source as possibly the first observation of the site of particle acceleration in a solar flare remains. Whether thermal or non-thermal, both models require that energisation of the particles take place at the loop-top, and it is probably this energisation site which we see.

Acknowledgements. I am pleased to thank Jan Kuijpers of the Sterrekundig Instituut, Utrecht for useful discussion and comments, and wish to acknowledge the support of EC Lab-Twinning Contract SCI*-CT91-0727.

References

Achterberg, A. and Krülls, W.:1992, Astron.Astrophys. 265, L13.
Fletcher, L and Brown, J.C.: 1995, Astron. Astrophys. 294, 260
Gardiner, C.W.:1985 in H.Haken (ed.), Handbook of Stochastic Methods.
Machado, M., Avrett, E.H., Vernazza, J.E. and Noyes, R.W.: 1980, Ap.J. 242, 336.
MacKinnon, A.L. and Brown, J.C.: 1990, Astron.Astrophys. 232, 544.
MacKinnon, A.L. and Craig, I.J.D.:1991, Astron.Astrophys. 251, 693.
Masuda,S., Kosugi, T., Hara, H., Tsuneta, S. and Ogawara, Y.: 1994, Nature 371, 495.
Masuda,S.:1994, Ph.D. Thesis, University of Tokyo.
van den Oord, G.H.J.: 1990, Astron.Astrophys. 234, 496

This article was processed by the author using Springer-Verlag LaTeX A&A style file *L-AA* version 3.